

# Rejecting noise in Baikal-GVD data with neural networks

---

I. Kharuk,<sup>a,b</sup> G. Rubtsov,<sup>a,c</sup> G. Safronov<sup>a,d</sup>

<sup>a</sup>*Institute for Nuclear Research of the Russian Academy of Sciences,  
60th October Anniversary Prospect, 7a, Moscow, 117312, Russia*

<sup>b</sup>*Moscow Institute of Physics and Technology,  
Institutsky lane 9, Dolgoprudny, Moscow region, 141700, Russia*

<sup>c</sup>*Novosibirsk State University,  
Novosibirsk, 630090, Russia*

<sup>d</sup>*Joint Institute for Nuclear Research,  
Joliot-Curie 6, Dubna, Moscow Region, 141980, Russia*

*E-mail:* [ivan.kharuk@phystech.edu](mailto:ivan.kharuk@phystech.edu)

ABSTRACT: Baikal-GVD is a large ( $\sim 1 \text{ km}^3$ ) underwater neutrino telescope installed in the fresh waters of Lake Baikal. The deep lake water environment is pervaded by background light, which produces detectable signals in the Baikal-GVD photosensors. We introduce a neural network for an efficient separation of these noise hits from the signal ones, stemming from the propagation of relativistic particles through the detector. The neural network has a U-net like architecture and employs temporal (causal) structure of events. On Monte-Carlo simulated data, it reaches 99% signal purity (precision) and 98% survival efficiency (recall). The benefits of using neural network for data analysis are discussed, and other possible architectures of neural networks, including graph based, are examined.

---

## Contents

<b>1</b>	<b>Introduction</b>	<b>1</b>
<b>2</b>	<b>Monte-Carlo simulations</b>	<b>2</b>
<b>3</b>	<b>Neural network architecture</b>	<b>3</b>
3.1	Data representation	3
3.2	Neural network architecture	5
<b>4</b>	<b>Results</b>	<b>6</b>
<b>5</b>	<b>Conclusion</b>	<b>8</b>
<b>A</b>	<b>Graph neural network</b>	<b>8</b>

---

## 1 Introduction

Baikal-GVD is a neutrino telescope aimed at studying neutrino astrophysics [1]. It is currently under construction in Lake Baikal, Russia, and will have an effective volume of approximately 1 km<sup>3</sup>. The experiment’s mission, similar to other large volume neutrino telescopes [2–4], includes the measurements of neutrino flux, energy spectrum, and identification of neutrino sources.

The basic components of the Baikal-GVD detector are optical modules (OMs) accommodating a 10-inch high quantum efficiency photomultipliers (Hamamatsu R7081-100). They are aimed at registering the Cherenkov light from relativistic particles (originating from cosmic neutrinos and air showers) in the effective volume of the detector. OMs are carried by *strings* (36 OMs per string) and are located at a depth of 750 to 1275 meters with a 15-meter spacing. The strings are organized into *clusters* – approximately regular heptagons with a string in the middle, see Fig. 1. In total, there are 10 clusters with an average distance of 300 meters between the clusters and an average cluster radius of 60 meters.

As OMs are located underwater, they are subject to the natural luminescence of the Baikal water [5]. This causes random, uncorrelated activations of OMs, which constitute background (noise) hits in the data. These noise hits have the rate of 20–100 kHz (depending on depth and season), and their charge deposition is at the level of 1 photo-electron (p.e.). On average, noise hits constitute approximately 85–90% of the data collected for the analysis.

The characteristics of noise hits are similar to the weakest signal hits originating due to the propagation of relativistic particles through the detector. To reliably estimate the

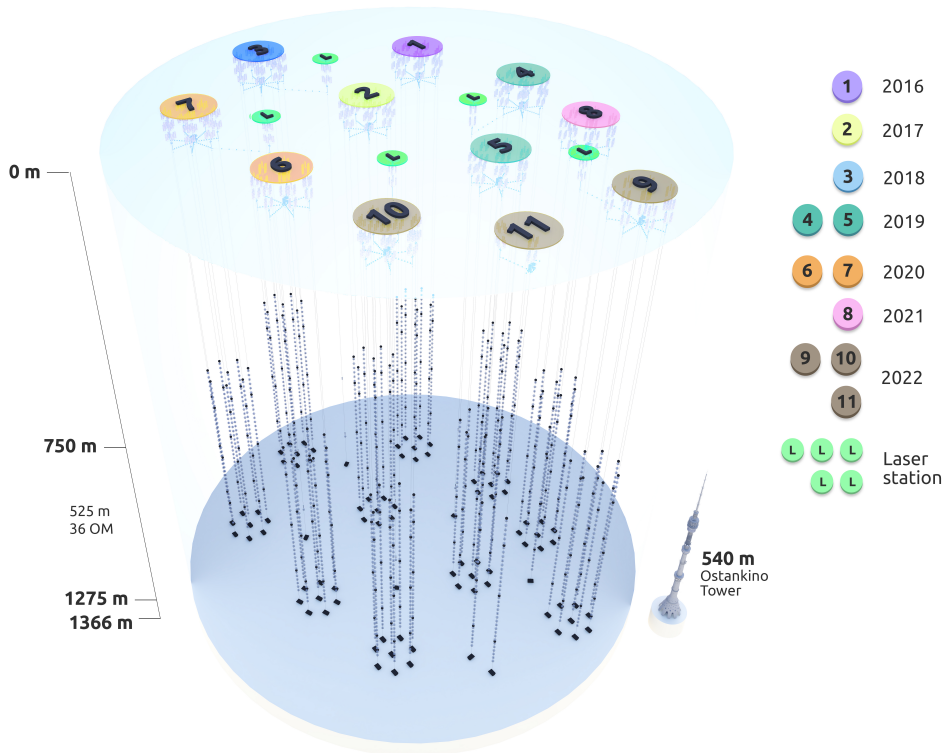


**Figure 1.** Schematic representation of the Baikal-GVD detector.

energy and incoming direction of a detected particle, these noise and signal hits must be differentiated. Also, a strong filtering algorithm will allow one to efficiently distinguish between neutrino-induced and atmospheric muon bundle-induced events. This necessitates the need for an effective filtering algorithm.

In this paper we present a neural network developed for rejecting the background in a standalone cluster readout regime. As compared to the noise suppression algorithms developed by the Baikal-GVD collaboration [1, 6], this machine-learning based approach improves the quality of signal-noise separation and allows for a much faster data analysis. The method can also be readily extended to process the multi-cluster data.

The paper is structured as follows. In section 2 we describe the Monte-Carlo simulations. In section 3 the neural network architecture and data representation are discussed. The results, including comparison with non-machine learning methods, are presented in section 4. Finally, section 5 concludes the paper.

## 2 Monte-Carlo simulations

Simulation of the data is performed via the Monte-Carlo method. Two types of incoming particles are considered: 1) muon neutrinos arriving from under the horizon, and 2) bundles of muons originating from cosmic air showers. The energy spectrum and in-

coming directions of arriving particles are chosen to coincide with the one expected in the experiment, see [7, 8] for details. The procedure takes into account photon scattering in the Baikal water and full simulation of cosmic air showers' evolution using QGSJET [9] and CORSIKA [10]. The noise rate and charge distribution are simulated so as to mimic the experimentally observed detector conditions.

The triggering condition for identifying an *event* is the following: two adjacent OMs, within the 100 ns time window, register signals that are at least 4.5 and 1.5 p.e. If this condition is fulfilled, the data from all OMs exceeding the signal-level threshold (0.3 p.e.) is collected for further analysis.

Registered signals (waveforms) are approximated by discrete hits (pulses). Each of the hits is characterized by the following physical observables:

1. Time at which the hit was registered,
2. Integral charge (in p.e.) registered by OM,
3. Maximal amplitude of the registered signal.

Additionally, in Monte-Carlo simulated data each hit is supplemented by a label indicating its origin. We reduced these labels to a binary mask indicating whether a given hit was due to the propagation of a relativistic particle (signal hit) or due to the water luminescence (noise hit). This allows us pose the problem of rejecting the background noise as a supervised segmentation task, i.e. predicting whether a given hit in an event represents a noise or a signal.

For training the neural network, we used neutrino-induced and cosmic ray-induced events. To avoid bias related to different signatures of these two types of events, we took an equal number of samples of both types, approximately  $10^6$  entries each. It was observed that neural network metrics on both types of events are similar, and that changing the proportion does not significantly affect the results. The data have been split into train, validation, and test sets in proportion 8/1/1.

### 3 Neural network architecture

#### 3.1 Data representation

Performance of a neural network strongly depends on a way the data is represented (sequence, image, graph). Hence it is of primary importance to choose the most efficient representation. For Baikal-GVD, we have three possible options:

1. Organize data in a three dimensional array mimicking geometrical structure of the cluster;
2. Make a sequence by ordering the hits according to their activation times, thus exploiting temporal (causal) structure of the events;
3. Consider each event as a graph.

In what follows we refer to these options as geometrical, temporal, and graph representations correspondingly. Variations and combinations of these representations have been applied for data analysis in physical experiments [11–15], including neutrino telescopes [16–18]. Below we comment on each of the possibilities one by one, highlighting their pros and cons for our task. In each case, the information on hits is given by the following 5 parameters:

- 1) Integral charge registered by OM during a pulse;
- 2) Time the hit was registered at;
- 3-5) x, y, and z coordinates of the corresponding OM.

In the geometrical approach, we have introduced a  $3 \times 3 \times 36$  array mimicking geometrical structure of a cluster (plus one auxiliary string). This representation has a drawback: one can store only one OM activation per event, which might result in a loss of signal hits. This can be resolved by introducing an additional time axis, as it was done in [4]. However, this is highly memory-demanding, and we decided to keep only the activation with the highest integral signal.

To analyze the data, we used a ResNet-like neural network [19] – a convolution-based neural network with residual connections often used for image classification and segmentation. However, its performance turned out to be 1-2% worse than that of the best solution. Combined with the abovementioned drawback, we decided not to develop this approach further.

For the graph representation of the data, we have developed a graph neural network of the message passing type [20] with a modification of the attention mechanism [21]. We have also implemented a non-standard message parsing algorithm utilizing temporal ordering of the activations. The details on data representation and graph updating protocol are given in the appendix A. The performance of this neural network was compatible with the best solution, but was much more memory demanding.

The best results were obtained by utilizing the temporal representation of the data. Namely, for a given event, all of the hits were ordered according to their activation times. As the number of activated OMs varies from event to event, we fixed all events to have exactly 112 hits by adding auxiliary hits (filled with zeros), if needed. We also made a mask channel to keep track of these auxiliary hits. Thus, each event was represented by a  $112 \times (5+1)$  array. Neural network’s architecture is described in detail in the next section.

We believe that temporal representation works best, as in this case signal hits form clusters, which allows the neural network to efficiently identify them. For other tasks the best data representation might be different. For example, for the reconstruction of neutrinos’ arriving direction geometrical properties of an event are expected to be more important than its causal structure. Correspondingly, geometrical and graph representations of the data are expected to be more suitable for this task.

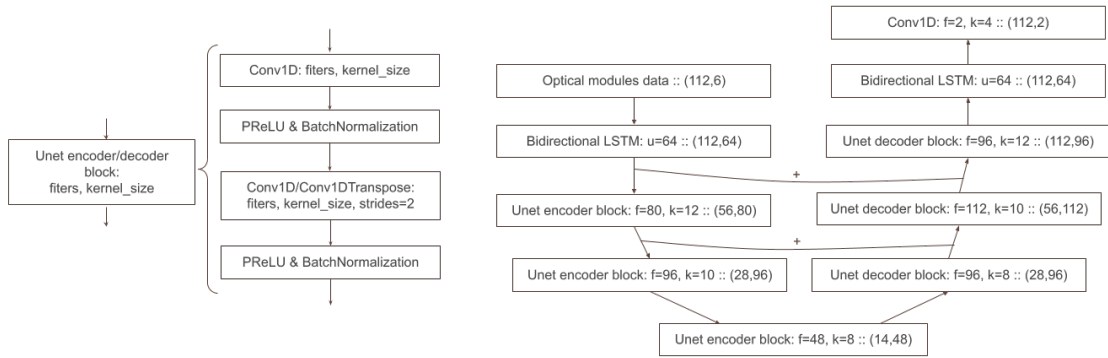


**Figure 2.** Architecture of the neural network. Arrows show the data flow, plus sign indicates concatenation of the data.

### 3.2 Neural network architecture

One of the neural network architectures known to be well suited for segmentation tasks is the U-net [14, 22–24]. Its power comes from the fact that it utilizes both global and local information. Namely, convolutions without dimensionality reduction (U-net encoder blocks, fig. 2) provide local information for a given OM from the neighboring cells. Convolutions with dimensionality reduction followed by transposed convolutions (U-net decoder blocks) have significantly larger receptive field. This provides the neural network with the information on global features of an event as well. Combining these two types of information allows for an effective segmentation of the data. This was our motivation for choosing the U-net as a basic neural network architecture.

We found it beneficial to add two bidirectional long short-term memory (LSTM) cells [25], one prior and one after the U-net. Recurrent units, such as LSTM, are designed for analyzing sequences [26–28]. Thus, by adding these additional layers, we made use of the fact that the data is provided in the form of a sequence.

The last layer of the neural network is a convolution block with softmax activation function. Its output is a number  $c \in [0; 1]$  representing neural network’s confidence on whether a given hit is a signal one. By setting a threshold  $c_0$ , all hits can be binary split into signal and noise hits.

Full architecture of the neural network is presented on Fig. 2.

We have also tried training neural networks based solely on LSTM cells or convolution blocks without dimensionality reduction. Their performance was slightly worse.

We used TensorFlow [29] to implement the neural network. For training, we employed Adam optimizer [30] with a dynamical learning rate and used early stopping to avoid overfitting. The activation functions were chosen as follows: PReLU [31] in the U-net block, hyperbolic tangent in LSTM cells, and softmax in the last layer of the neural network. The training takes approximately 36 hours on NVIDIA RTX 3090.

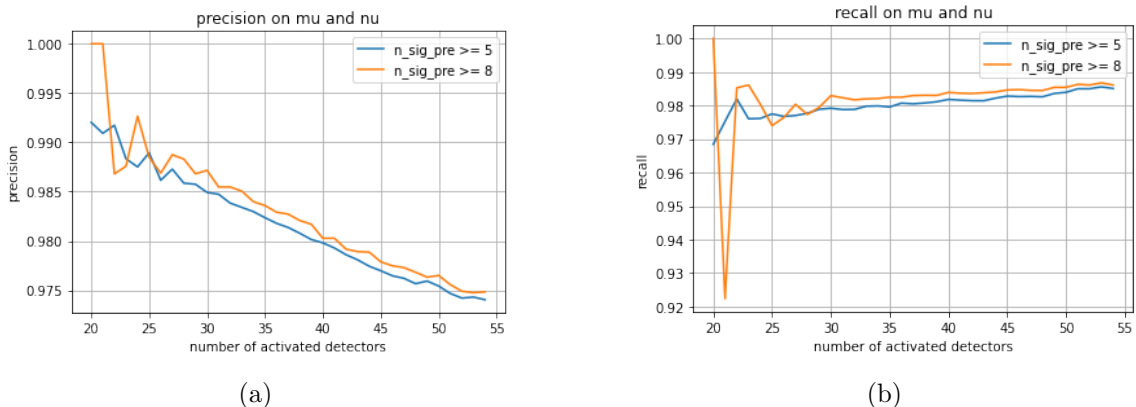


**Figure 3.** Plots of the dependence of precision (a) and recall (b) as functions of the number of registered hits in an event. Blue and orange curves correspond to events with at least 5 and 8 signal hits correspondingly.

## 4 Results

Neural network’s performance was evaluated using the standard metrics – signal purity (precision) and survival efficiency (recall). The metrics were estimated on the test dataset, which is an equal-part mixture of neutrino-induced and muon bundle-induced events. Figure 3 illustrates the dependence of the metrics on the number of registered hits in an event for the identification threshold of  $c_0 = 0.5$ . As it can be expected, the neural network performs slightly better on events with a higher fraction of signal hits. The metrics evaluated on neutrino-induced events only are very close to the ones presented on Fig. 3.

By changing the threshold value, one can adjust the relation between precision and recall. This is important, for instance, for reconstructing the arrival direction of a detected particle, when it is important to get the highest possible signal purity. Figure 4 demonstrates that one can get higher signal purity at the cost of lower survival efficiency. Another way to adjust the metrics is to assign weights for the signal and noise hits during the training phase of the neural network. We observed that this slightly increases precision (by 0.4%), while recall becomes significantly worse (by 3%).

Neural network’s response matrix for the reconstructed versus true number of signal hits is presented on Fig. 5 for the classification threshold of 0.7. The functional dependence between the parameters can be approximated by a straight line. As the number of signal hits and event energy are correlated, this implies that neural network’s predictions are reliable in the whole range of energy spectrum.

The identification of OMs activation time is subject to calibration and instrumental errors. As our neural network strongly relies on the temporal ordering of the events, we have checked the robustness of our approach with respect to hit time measurement uncertainty. Namely, we have perturbed the activation times of all OMs using the normal distribution with the standard deviation of 3 ns (the expected error is 3–5 ns). In the worst case scenario, when all of the time shifts are independent, the metrics become 1% worse. We consider this to be a minor change, and thus claim our method to be robust.

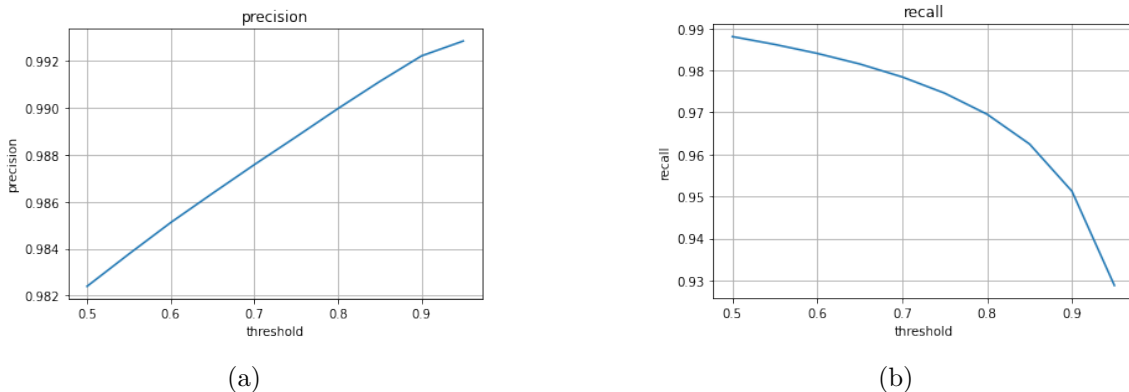


**Figure 4.** Dependence of precision (a) and recall (b) as the function of the threshold value.

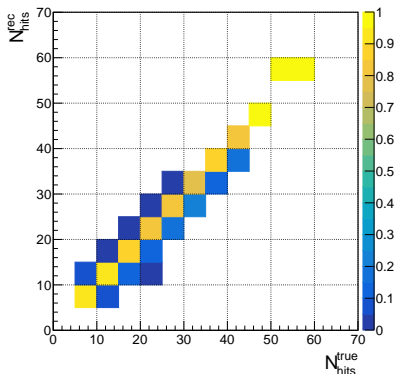


**Figure 5.** Response matrix for the number of reconstructed signal hits. The number of true and reconstructed signal hits are given on horizontal and vertical axes correspondingly.

As compared to non-machine learning based approach (algorithmic) to rejecting the noise [1, 6], the metrics of the neural network are several percents better. Moreover, the developed approach allows for a much faster data analysis.

We have performed the cross-analysis of the events processed by the neural network and by the standard track fitting algorithm [7] using Baikal-GVD muon reconstruction software. Namely, on the test MC sample of the atmospheric neutrinos, the signal hits identified by both methods were used to estimate the angular resolution. The resulting error was found to be similar for both approaches. We expect that the combination of the developed neural network with a machine learning-based or maximum likelihood-based reconstruction algorithm will reduce the reconstruction error.

We have also examined the applicability of the neural network to the analysis of the real experimental data collected during one of the 2019 season runs. Signal hits, identified by the neural network in the data, were passed them through the Baikal-GVD muon reconstruction software. The comparison of various distributions showed general agreement between data and MC. However, some of the discrepancies require further study before the neural network can be routinely applied to the data.

## 5 Conclusion

We have presented the neural network for rejecting the noise in the Baikal-GVD experiment. Its main feature is that it utilizes temporal (casual) structure of events. The neural network shows better metrics than the standard algorithmic approach, and allows for a much faster data analysis. Also, after minor changes, it can be used for a more detailed segmentation of events – into track-like, cascade-like, and noise hits.

This work constitutes the first step towards introducing a full cycle of machine learning-based data analysis for the Baikal-GVD experiment. Namely, we are developing neural networks for an effective separation of neutrino-induced and muon bundle-induced events, their energy and arrival direction reconstruction. It is expected that the introduction of these neural networks will further improve data analysis quality.

## Acknowledgments

The work is supported by the Russian Science Foundation grant number 22-22-20063.

## A Graph neural network

Graph neural networks have been successfully applied for solving various tasks [3, 11, 12, 20], including data analysis of neutrino telescopes [17, 32]. This motivated us to develop a graph neural network for the purpose of rejecting the noise.

We considered OMs as vertices of a graph. Each vertex has 6 parameters described in the main part of the paper. We assumed the initial graph to be fully connected. This is motivated by the fact that it is *a priori* unknown which OMs are relevant for determining whether a given hit is a signal one or not. A simpler approach is to connect only  $k$  nearest neighbors, chosen according to the temporal ordering of OMs. This yields comparable yet slightly worse results.

We have chosen our neural network to be of the message passing type as they have most general, and hence powerful, architecture. Let us explain the data analysis protocol step by step, following the data flow in the neural network. Unless otherwise stated, the activation function of a layer is the scaled exponential linear unit.

1) *Nodes encoding*. At the first step of data analysis, we update the encodings of the vertices. This is done via a dense layer with 48 units, which updates each of the vertices encodings independently.

2) *Messages creation*. Further, we prepare messages between each pair of the vertices. This is done in a usual manner – by a dense layer with 48 units that takes as input the encodings of two nodes and outputs a message from one node to another.

3) *Attention mechanism*. At the next step, the obtained messages are multiplied by the corresponding values of the adjacency matrix. The idea is that we consider adjacency matrix as the attention mechanism, which leaves only relevant messages. The updating rule of the adjacency matrix is given below.

4) *Message parser*. To obtain a single message for a vertex, we order all messages sent to a given vertex according to the activation times of the corresponding OMs (temporal

ordering). This sequence is passed via a convolutional layer (48 filters, kernel size 5, strides 2), followed by a maxpooling layer (strides 2). The motivation behind this procedure is to make use of a physically meaningful ordering of the vertices – the temporal one. To obtain a single message, we sum the processed messages and divide the result by the sum of values in the adjacency matrix at the corresponding row.

5) *Nodes updating.* Further, vertices encodings are updated using a dense layer with 48 units. This layer takes as input current encoding of the vertex and the relevant message.

6) *Adjacency matrix updating.* Finally, we update the adjacency matrix. Namely, we form all possible pairs of the vertices and pass them through a dense layer with 48 units and sigmoid activation function. The resulting output is interpreted as the mutual relevance of the cells. Such interpretation is supported by the fact that, upon examination of the adjacency matrix, it tends to have non-zero entries only between signal hits. Note that at the 2nd step we consider all possible pairing of the vertices, independently of the values of the adjacency matrix.

The described steps of data analysis constitute a single layer of our graph neural network. To get best results, we stacked 4 such layers on top of each other. The output of the last layer is passed through a dense layer with one output unit and the sigmoid activation function. This yields the neural network’s confidence on whether a given hit is a signal one.

We believe that the reason why the performance of the graph neural network wasn’t better than that of the convolutional one is the following. Graph neural networks allow one to work with data that can be represented in a form of a graph. For the case at hand, this is not needed, as there is a useful and physically meaningful representation of the data – temporal one. This allows neural network to understand the structure of the data, yielding graph representation unnecessary.

## References

- [1] I. Belolaptikov, Z. Dzhilkibaev et al., *Neutrino telescope in lake baikal: Present and nearest future*, *arXiv preprint arXiv:2109.14344* (2021) .
- [2] ICECUBE collaboration, M. G. Aartsen et al., *Evidence for High-Energy Extraterrestrial Neutrinos at the IceCube Detector*, *Science* **342** (2013) 1242856, [1311.5238].
- [3] S. Adrián-Martínez, A. Albert, M. André, M. Anghinolfi, G. Anton, M. Ardid et al., *Searches for point-like and extended neutrino sources close to the galactic center using the antares neutrino telescope*, *The Astrophysical journal letters* **786** (2014) L5.
- [4] S. Aiello, S. Akrame, F. Ameli, E. Anassontzis, M. Andre, G. Androulakis et al., *Sensitivity of the km<sup>3</sup>net/arca neutrino telescope to point-like neutrino sources*, *Astroparticle Physics* **111** (2019) 100–110.
- [5] A. Avrorin, A. Avrorin, V. Aynutdinov, R. Bannash, I. Belolaptikov, V. Brudanin et al., *The optical noise monitoring systems of lake baikal environment for the baikal-gvd telescope*, *arXiv preprint arXiv:1908.06509* (2019) .

- [6] V. Allakhverdyan, A. Avrorin, A. Avrorin, V. Aynutdinov, R. Bannasch, Z. Bardačová et al., *An efficient hit finding algorithm for baikal-gvd muon reconstruction*, *arXiv preprint arXiv:2108.00208* (2021) .
- [7] V. Allakhverdyan, A. Avrorin, A. Avrorin, V. Aynutdinov, R. Bannasch, Z. Bardačová et al., *Measuring muon tracks in baikal-gvd using a fast reconstruction algorithm*, *The European Physical Journal C* **81** (2021) 1–9.
- [8] J. Stasielak, P. Malecki, D. Naumov, V. Allakhverdian, A. Karnakova, K. Kopański et al., *High-energy neutrino astronomy—baikal-gvd neutrino telescope in lake baikal*, *Symmetry* **13** (2021) 377.
- [9] N. Kalmykov and S. Ostapchenko, *The nucleus-nucleus interaction, nuclear fragmentation, and fluctuations of extensive air showers*, *Physics of Atomic Nuclei* **56** (1993) 346–353.
- [10] D. Heck, J. Knapp, J. Capdevielle, G. Schatz, T. Thouw et al., *Corsika: A monte carlo code to simulate extensive air showers*, *Report fzka* **6019** (1998) .
- [11] F. Drielsma, Q. Lin, P. C. de Soux, L. Dominé, R. Itay, D. H. Koh et al., *Clustering of electromagnetic showers and particle interactions with graph neural networks in liquid argon time projection chambers*, *Physical Review D* **104** (2021) 072004.
- [12] T. Bister, M. Erdmann, J. Glombitza, N. Langner, J. Schulte and M. Wirtz, *Identification of patterns in cosmic-ray arrival directions using dynamic graph convolutional neural networks*, *Astroparticle Physics* **126** (2021) 102527.
- [13] O. Kalashev, I. Kharuk, M. Kuznetsov, G. Rubtsov, T. Sako, Y. Tsunesada et al., *Deep learning method for identifying mass composition of ultra-high-energy cosmic rays*, *Journal of Instrumentation* **17** (2022) P05008.
- [14] L. Dominé, P. C. de Soux, F. Drielsma, D. H. Koh, R. Itay, Q. Lin et al., *Point proposal network for reconstructing 3d particle endpoints with subpixel precision in liquid argon time projection chambers*, *Physical Review D* **104** (2021) 032004.
- [15] L. Dominé, K. Terao, D. Collaboration et al., *Scalable deep convolutional neural networks for sparse, locally dense liquid argon time projection chamber data*, *Physical Review D* **102** (2020) 012005.
- [16] S. Aiello, A. Albert, S. A. Garre, Z. Aly, F. Ameli, M. Andre et al., *Event reconstruction for km<sup>3</sup>net/orca using convolutional neural networks*, *Journal of Instrumentation* **15** (2020) P10005.
- [17] N. Choma, F. Monti, L. Gerhardt, T. Palczewski, Z. Ronaghi, P. Prabhat et al., *Graph neural networks for icecube signal classification*, in *2018 17th IEEE International Conference on Machine Learning and Applications (ICMLA)*, pp. 386–391, IEEE, 2018.
- [18] M. Huenefeld, *Deep learning in physics exemplified by the reconstruction of muon-neutrino events in icecube*, *Verhandlungen der Deutschen Physikalischen Gesellschaft* (2017) .
- [19] K. He, X. Zhang, S. Ren and J. Sun, *Deep residual learning for image recognition*, in *Proceedings of the IEEE conference on computer vision and pattern recognition*, pp. 770–778, 2016.
- [20] J. Gilmer, S. S. Schoenholz, P. F. Riley, O. Vinyals and G. E. Dahl, *Neural message passing for quantum chemistry*, in *International conference on machine learning*, pp. 1263–1272, PMLR, 2017.

- [21] P. Veličković, G. Cucurull, A. Casanova, A. Romero, P. Lio and Y. Bengio, *Graph attention networks*, *arXiv preprint arXiv:1710.10903* (2017) .
- [22] J. Long, E. Shelhamer and T. Darrell, *Fully convolutional networks for semantic segmentation*, in *Proceedings of the IEEE conference on computer vision and pattern recognition*, pp. 3431–3440, 2015.
- [23] O. Ronneberger, P. Fischer and T. Brox, *U-net: Convolutional networks for biomedical image segmentation*, in *International Conference on Medical image computing and computer-assisted intervention*, pp. 234–241, Springer, 2015.
- [24] Z. Zhou, M. M. Rahman Siddiquee, N. Tajbakhsh and J. Liang, *Unet++: A nested u-net architecture for medical image segmentation*, in *Deep learning in medical image analysis and multimodal learning for clinical decision support*, pp. 3–11. Springer, 2018.
- [25] S. Hochreiter and J. Schmidhuber, *Long short-term memory*, *Neural computation* **9** (1997) 1735–1780.
- [26] A. Aab, P. Abreu, M. Aglietta, J. Albury, I. Allekotte, A. Almela et al., *Extraction of the muon signals recorded with the surface detector of the pierre auger observatory using recurrent neural networks*, *Journal of Instrumentation* **16** (2021) P07016.
- [27] D. Bahdanau, K. Cho and Y. Bengio, *Neural machine translation by jointly learning to align and translate*, *arXiv preprint arXiv:1409.0473* (2014) .
- [28] I. Sutskever, O. Vinyals and Q. V. Le, *Sequence to sequence learning with neural networks*, *Advances in neural information processing systems* **27** (2014) .
- [29] M. Abadi, P. Barham, J. Chen, Z. Chen, A. Davis, J. Dean et al., *Tensorflow: A system for large-scale machine learning*, in *12th symposium on operating systems design and implementation (16)*, pp. 265–283, 2016.
- [30] D. P. Kingma and J. Ba, *Adam: A method for stochastic optimization*, *arXiv preprint arXiv:1412.6980* (2014) .
- [31] K. He, X. Zhang, S. Ren and J. Sun, *Delving deep into rectifiers: Surpassing human-level performance on imagenet classification*, in *Proceedings of the IEEE international conference on computer vision*, pp. 1026–1034, 2015.
- [32] S. Reck, D. Guderian, G. Vermariën, A. Domi, K. Collaboration et al., *Graph neural networks for reconstruction and classification in km3net*, *Journal of Instrumentation* **16** (2021) C10011.